



Published in final edited form as:

*Cancer Discov.* 2011 December 1; 1(7): 580–586. doi:10.1158/2159-8290.CD-11-0215.

## A novel platform for detection of CK+ and CK– CTCs

Chad V. Pecot<sup>1,\*</sup>, Farideh Z. Bischoff<sup>2,\*</sup>, Julie Ann Mayer<sup>2</sup>, Karina L. Wong<sup>2</sup>, Tam Pham<sup>2</sup>, Justin Bottsford-Miller<sup>3</sup>, Rebecca L. Stone<sup>3</sup>, Yvonne G. Lin<sup>3</sup>, Padmavathi Jaladurgam<sup>3</sup>, Ju Won Roh<sup>3,9</sup>, Blake W. Goodman<sup>3</sup>, William M. Merritt<sup>3</sup>, Tony J. Pircher<sup>2</sup>, Stephen D. Mikolajczyk<sup>2</sup>, Alpa M. Nick<sup>3</sup>, Joseph Celestino<sup>3</sup>, Cathy Eng<sup>4</sup>, Lee M. Ellis<sup>6,7</sup>, Michael T. Deavers<sup>5</sup>, and Anil K. Sood<sup>3,7,8</sup>

<sup>1</sup>Division of Cancer Medicine, The University of Texas MD Anderson Cancer Center, Houston, Texas, USA

<sup>2</sup>Biocept Inc., San Diego, California, USA

<sup>3</sup>Department of Gynecologic Oncology, The University of Texas MD Anderson Cancer Center, Houston, Texas, USA

<sup>4</sup>Department of Gastrointestinal Medical Oncology, The University of Texas MD Anderson Cancer Center, Houston, Texas, USA

<sup>5</sup>Department of Pathology, The University of Texas MD Anderson Cancer Center, Houston, Texas, USA

<sup>6</sup>Department of Surgical Oncology, The University of Texas MD Anderson Cancer Center, Houston, Texas, USA

<sup>7</sup>Center for RNA Interference and Non-Coding RNA, The University of Texas MD Anderson Cancer Center, Houston, Texas, USA

<sup>8</sup>Department of Cancer Biology, The University of Texas MD Anderson Cancer Center, Houston, Texas, USA

<sup>9</sup>Department of Obstetrics & Gynecology, Dongguk University Ilsan Hospital, 814, Shicsa-dong, Ilsandong-gu, Goyang, Korea 411-773

### Abstract

Metastasis is a complex, multistep process that begins with the epithelial-mesenchymal transition (EMT). Circulating tumor cells (CTCs) are believed to have undergone EMT and thus lack or express low levels of epithelial markers commonly used for enrichment and/or detection of such cells. However, most current CTC detection methods only target EpCAM and/or cytokeratin to enrich epithelial CTCs, resulting in failure to recognize other, perhaps more important, CTC phenotypes that lack expression of these markers. Here, we describe a population of complex aneuploid CTCs that do not express cytokeratin or CD45 antigen in patients with breast, ovarian, or colorectal cancers. These cells were not observed in healthy subjects. We show that the primary epithelial tumors were characterized by similar complex aneuploidy, indicating conversion to an EMT phenotype in the captured cells. Collectively, our study provides a new method for highly efficient capture of previously unrecognized populations of CTCs.

---

Correspondence should be addressed to A.K.S. (asood@mdanderson.org). Departments of Gynecologic Oncology and Cancer Biology, The University of Texas MD Anderson Cancer Center, Unit 1362, PO Box 301439, Houston, TX 77230-1439.

\*These authors contributed equally to this work.

**Conflict of interest statement:** The authors F.Z.B., T.J.P., S.D.M., J.A.M., K.W., and T.P. are employees of Biocept Incorporated.

**Significance**—Current assays for CTC capture likely miss populations of cells that have undergone EMT. Capture and study of CTCs that have undergone EMT would allow a better understanding of the mechanisms driving metastasis.

---

## INTRODUCTION

An epithelial-mesenchymal transition (EMT) in cancer is characterized by loss of cell adhesion, repression of E-cadherin, acquisition of mesenchymal markers, increased cell motility, and invasive potential (1). Though several approaches describing alternative strategies for recovery and detection of CTCs have been reported, the only FDA-approved technique for CTC detection relies on the use of antibodies targeting the epithelial cell adhesion molecule (EpCAM), followed by cytokeratin (CK) and CD45 staining to confirm an epithelial phenotype (2, 3). These modern enrichment techniques have characterized such CTCs, showing correlation with survival (4–6) and response to treatment (6, 7). CTCs can also express biomarkers reflective of the primary tumor and could be useful as a surrogate for tumor biopsy (8, 9). However, only a small proportion of CTCs are capable of establishing distant metastasis (10, 11) as evidenced by the phenotypic heterogeneity observed among CTCs within patient blood samples (8). Biological mechanisms, such as EMT, may also result in a spectrum of epithelial marker shedding and a more progressive metastatic phenotype. Yet, these important EMT-derived CTC populations are likely missed by current techniques (12). In fact, one of the initial reports describing EpCAM levels in various cancer types found that nearly all epithelial tumors have high expression, while tumors of mesenchymal lineage such as melanomas and sarcomas have no expression (13). It is unknown whether the most invasive and metastasis-primed cells that have undergone EMT (resembling a more mesenchymal phenotype) no longer express EpCAM and/or cytokeratin and thus evade detection with traditional techniques. Importantly, the relative paucity of clinical evidence that such a process exists has called the theory of EMT into question (14). Thus, the ability to capture post-EMT cells in circulation could have implications for studying the metastatic process as well as clinical management of cancer patients.

## RESULTS

### Capture of Carcinoma Cells Independent of EpCAM Expression

We have developed a microfluidic-based system for capture and analysis of rare cells in circulation, including CTCs (Supplementary Fig. 1a). The platform is capable of capturing rare cells from blood for subsequent molecular characterization directly within a uniquely designed microchannel (Supplementary Fig. 1b,c). Each microchannel consists of a roughly rectangular chamber (40 mm × 12 mm × 55 μm) in which approximately 9,000 variable diameter posts are randomly placed to disrupt laminar flow and maximize the probability of contact between target cells and the streptavidin-derivatized posts, resulting in their capture (15). The platform is versatile, permitting assay optimization with flexibility in the number of antibodies selected for capture and detection as well as allowing immediate and direct single-cell microscopic analyses through the transparent microchannel without the need to manipulate cells onto glass slides. This approach utilizes an antibody cocktail that is added directly to cells prior to capture, enabling recovery of variable CTC phenotypes. Briefly, this mixture contains antibodies directed towards a variety of epithelial cell surface antigens (EpCAM, HER2, MUC1, EGFR, folate binding protein receptor, TROP-2), and mesenchymal or stem cell antigens (c-MET, N-Cadherin, CD318 and mesenchymal stem cell antigen). Each of these antibodies was tested by flow cytometry for reactivity to several well-characterized cancer cell lines (e.g., SKOV3, LNCaP, SKBR3) and shown to be additive in binding to cells (Supplementary Fig. 2). Antibodies were tested to have minimal

cross-reactivity to nucleated cells in healthy control blood. Analytical control samples, namely blood from healthy donors spiked with cancer (SKOV3) cells, were run using this antibody mixture to ensure optimal performance in detecting tumor cells (based on CK staining).

Analytical validation of the platform to demonstrate precision, reliability, and reproducibility in recovery and detection of CTCs based on CK+/CD45-/DAPI+ (4', 6-diamidino-2-phenylindole) staining was performed with *ex vivo* spiking experiments of carcinoma cells into whole blood. Tumor cell capture efficiency was validated through a series of cell spiking experiments. We demonstrate analytical precision in recovery and detection of low- to high-EpCAM expressing target cells, independent of the number of cells spiked (Fig. 1a). We further show >95% reproducibility in tumor cell capture with several cell lines (Fig. 1b). Capture efficiency using the antibody cocktail was demonstrated with low (T24) and medium (SKOV3) EpCAM-expressing cell lines (16). While SKOV3 cells had high capture efficiency with EpCAM alone as well as with cocktail (>80%), T24 capture efficiency was markedly improved from <10% capture with EpCAM alone to >80% with antibody cocktail ( $P = 0.0001$ ; Fig. 1c).

Next, clinical verification of capture efficiency was tested by examining CTCs in patient samples. In the first cohort of 21 patients with advanced-stage disease, we compared CTC detection with our platform using either EpCAM alone or antibody cocktail (Supplementary Table 1). Improved recovery was observed with higher CTC numbers in 14 of 21 samples with the antibody cocktail ( $P = 0.07$ ). In 100 normal blood controls, only 1 CK+/CD45-/DAPI+ cell was detected, demonstrating high specificity of the staining procedure. In the second, larger cohort of 93 patients with advanced-stage lung, breast, colorectal or prostate cancer, we compared CellSearch® and our platform using the antibody cocktail for capture. Based on standard CK+/CD45-/DAPI+ stain criteria, our platform was found to be significantly more sensitive for CTC enumeration in colorectal, prostate and lung cancers (Fig. 1d).

### Capture and Detection of CK- CTCs in Patients with Breast, Ovarian or Colorectal Cancers

Given that CK expression levels can often be variable among epithelial cells and absent among other non-epithelial cell types, we examined CK staining efficiency within the microchannel using a third cohort of *HER2-neu* positive breast cancer samples (n=19) for which fluorescence *in situ* hybridization (FISH) analysis of the *HER2* locus enabled confirmation of CTC recovery independent of CK/CD45 staining (Fig. 2a). CK+ cells were located in each of the 19 cases and used as target cells for analysis of *HER2* by FISH. In addition, all CK-/CD45- cells were also classified as “possible” CTCs for subsequent analysis of *HER2* signals. In 18 of 19 cases (94.7%), a range of 0.04–2.4 *HER2*-amplified CTCs per mL blood were detected among the CK+/CD45- and CK-/CD45--classified cells, suggesting that the CK- *HER2*-amplified CTCs originated from the primary tumor. When excluding CK- *HER2*-amplified CTCs, only 12 (63.2%) of the patient samples were found to have CK+ *HER2*-amplified cells, which is consistent with other similar reports (17). Interestingly, only 24.3% of all CK+ CTCs were found to have *HER2-neu* amplification ( $P=0.007$ , Fig. 2b). Surprisingly, 49.7% of the *HER2*-amplified cells were CK- (Fig. 2b). These results demonstrate the inefficiency in detection of CTCs based solely on CK+/CD45- stain criteria, resulting in failure to detect a significant population of *HER2*-amplified cells. Thus, given the unique design and amenity to sequential staining and FISH, the platform enabled incorporation of FISH directly within the microchannel as a valuable independent method in confirming recovery of both CK+ and CK- CTCs immediately after CK staining.

To further confirm the use of the FISH-based strategy, we applied the same antibody cocktail capture approach and CTC detection (CK+/CD45-/DAPI+ staining) on samples from patients with advanced ovarian or colorectal cancer. To verify detection of CTCs, we again used FISH, but with the aim to detect aneuploidy (unbalanced genomic copy number changes). We rarely found CK+/CD45- stained cells; roughly 0.1 cells/mL blood of ovarian cancer patients regardless of stage, tumor grade, or CA-125 levels were CK+/CD45- (Supplementary Table 2). FISH probes targeted to frequently gained genomic regions in ovarian and colorectal carcinoma were chosen based on array comparative genomic hybridization data (18, 19). Each probe was first tested on a total of 2,500 normal peripheral blood cells from five donors and in CK+ cultured SKOV3 cells to determine hybridization efficiency and scoring accuracy in interphase cells captured within the microchannel (see Methods section). Cells that displayed only a monosomic signal for any one of the three probes were excluded (potential signal overlap). Therefore, only cells classified as either trisomic or complex aneuploid (at least one locus gain and another gain or loss at a second locus) were enumerated. As observed with the HER2-positive breast cancer cohort, for both ovarian and colorectal cancer, we found that not only captured CK+/CD45- cells (Fig. 2c), but also co-captured CK-/CD45- staining cells (Fig. 2d, Supplementary Tables 3,4) had complex aneuploidy. Complex aneuploidy was not observed among normal control blood samples. Similar to breast cancer, when assessing for frequency of complex aneuploidy, colorectal and ovarian cancer patients had nearly the same number of CK- as CK+ CTCs (Fig. 2e,f). Thus, the presence of CK- complex aneuploid cells further demonstrates the inefficiency of CK as a marker to detect all candidate CTCs.

### Cytokeratin-Negative CTCs Found within the Primary Tumor

We hypothesized that if the isolated CK- CTCs are the consequence of EMT then similar cells should be present within the primary tumor. We sought to verify that the circulating aneuploid cells identified in ovarian cancer patients had molecular features reflective of the primary tumor and, thus, are a useful population of CTCs. Blood was collected from 7 patients just before cytoreductive surgery. Multiple regions in the matched tumor and CTCs shared similar complex aneuploid patterns (Fig. 3a). Interestingly, about 20% of these aneuploid regions within the tumor were CK- and were heterogeneous in distribution (Fig. 3b). Although similar findings using FISH in CTCs and CECs compared to primary tumors have been described (20), these were based on circulating CK+ cells.

### Linking CK- CTCs to an Epithelial-Mesenchymal Transition

One possible mechanism giving rise to presence of CK- CTCs is EMT, a biological process reported to play a significant role in tumor progression and metastasis. Thus, there is growing interest in methods that enable capture and analysis of EMT-derived CTCs. To determine if our assay captures cells that have undergone EMT, we studied the effect of TGF- $\beta$  treatment on SKOV3 ovarian carcinoma cells. After 72 hours of treatment, CK staining was lost in about 20% of cells, correlating with an EMT morphologic change (Fig. 4a). Quantitative PCR analysis of these cells before and after TGF- $\beta$  treatment showed an increase in expression of mesenchymal markers (Fig. 4b). Cells, before and after treatment, were spiked *ex vivo* into mouse blood and run through the microchannel. All untreated cells captured were CK+; however, after TGF- $\beta$  treatment, 16% of the cells captured were CK- and had complex aneuploidy (Fig. 4c). Direct visualization of the FISH staining within the microchannel demonstrates these CK+ and CK- cells had nearly identical complex aneuploid patterns (Fig. 4d).

Next, to examine the utility of our CTC detection system for capturing tumor cells with EMT features in an *in vivo* setting, we studied the effect of TGF- $\beta$  treatment on HeyA8 ovarian carcinoma cells. After 72 hours of TGF- $\beta$  treatment, approximately 50–60% of cells

lost their CK staining (Fig. 4e). To determine if these CK<sup>-</sup> cells can be captured in circulation, we established a metastatic orthotopic model with HeyA8 cells. Ten tumor-bearing mice were monitored for signs of morbidity, at which point approximately 350  $\mu$ L of blood was obtained per mouse by cardiac puncture prior to sacrifice. All sites of metastatic tumor were carefully removed and weighed. Both CK<sup>+</sup> and CK<sup>-</sup> complex aneuploid CTCs were isolated from circulation within the microchannel (Fig. 4f). Enumeration of complex aneuploid CK<sup>-</sup> CTCs correlated with aggregate tumor burden (Fig. 4g).

## Discussion

Collectively, these results confirm the utility of our microfluidics platform as a reliable method for assay development and for efficient recovery of CTCs. We observed that a potentially important population of cancer cells is present in circulation that would likely be missed by standard detection criteria. Identification of the full spectrum of CTCs would permit more efficient and directed analysis among patient specimens where heterogeneous CTC populations are expected. Namely, detection of EMT-derived CTCs has been widely hypothesized as a population of cells that are missed by current platforms (12, 21). Our data suggest that these complex aneuploid CK<sup>-</sup> CTCs isolated in clinical samples may represent EMT-derived CTCs.

There are some recent reports of isolated CTCs expressing markers of EMT. For example, in metastatic breast cancer patients receiving standard therapies, CTCs correlated with more frequent expression of EMT markers (TWIST1, AKT2 and PI3K $\alpha$ ) in those who were resistant to treatment (22). Similar reports have found that CTCs can co-express both epithelial (CK and E-cadherin) and mesenchymal (vimentin and N-cadherin) markers (23, 24). Likewise, a higher incidence of CK<sup>+</sup>Vimentin<sup>+</sup> and CK<sup>+</sup>TWIST<sup>+</sup> CTCs was found in metastatic breast cancer patients versus women with earlier stage disease (25). These studies suggest a continuum in the spectrum of epithelial differentiation to mesenchymal phenotype, suggesting that CTCs may have a partial EMT phenotype (12). However, these platforms may miss clinically relevant populations of CTCs because they rely upon CK for CTC detection. To our knowledge, we provide the first report linking CK<sup>-</sup> CTCs to EMT.

Although the antibodies used in our study detect a wide range of CKs, it is possible that these antibodies may not detect all CKs. Thus, it is possible that the complex aneuploid CK<sup>-</sup> CTCs we detected may still express other CKs. There is increasing evidence that different CK antibodies detect different subsets of CTCs. Currently, different groups are targeting a variety of CKs for detection of CTCs, such as CK8, CK18 and CK19 (26–28) and CK7 and CK8 (2, 29). However, there is increasing concern that targeting only a few CKs for CTC detection, such as CK18 (30) or CK7, CK8, and CK18 (31) may fail to detect certain tumor cells. To target many different CTC phenotypes, our CK mix detects luminal (CK7, CK8, CK18, CK19) and basal (CK5, CK6, CK14, CK17) CTCs. While the pan-cytokeratin antibody used in our study has been successfully utilized by other groups (32), we added three additional cytokeratin antibodies (CK 7/17, CK18, and CK19) to the detection mix.

Interestingly, we observed similar ratios of total CK<sup>+</sup> CTCs to complex aneuploid CK<sup>+</sup> and CK<sup>-</sup>CTCs in three common cancer types. For example, only 24.3% of CK<sup>+</sup> CTCs in HER2/neu<sup>-</sup>positive breast cancer patients were found to have *HER2* amplification. There have now been multiple reports assessing the *HER2* status in CTCs from *HER2*-amplified breast cancer patients, most of which show a large proportion of captured CK<sup>+</sup> CTCs being negative for *HER2* amplification (33). This suggests that the classically defined CTC (CK<sup>+</sup>/CD45<sup>-</sup>/DAPI<sup>+</sup>) may over-represent cells that are of tumor origin. The FISH probes used in colorectal and ovarian cancer patients are unlikely to detect all CTCs with complex



aneuploidy, suggesting that some complex aneuploid CK<sup>+</sup> and CK<sup>-</sup> cells may still be missed. However, our platform allows for adaptability in selection of capture antibodies as well as use of different FISH probes and detection antibodies for immunofluorescence. Other investigators are now also exploring methods beyond the use of EpCAM and CK-based antibody platforms for capturing and detecting previously unrecognized CTC populations (34).

The platform presented here enables efficient assay development given the ability to interrogate all recovered cells for confirmation of success in targeted cell capture (i.e. detection of *HER2*-amplified CK<sup>-</sup> cells). While using only a limited number of FISH probes is unlikely to find all CK<sup>+</sup> and CK<sup>-</sup> cells with complex aneuploidy, more sophisticated interphase analysis may be considered. To the extent that CTCs represent a window into a patient's tumor, we present a new method for capturing and studying previously unrecognized CTC populations. Studies are clearly warranted to further classify distinct subtypes of CTCs. Further study of CK<sup>-</sup> CTCs may provide new insights into mechanisms of EMT and contribute to development of a clinically useful biomarker.

## METHODS

### Blood collection

Blood samples were drawn from patients with ovarian, peritoneal, fallopian tube, breast, or gastrointestinal cancers or benign pelvic tumors according to an Institutional Review Board-approved protocol at the M.D. Anderson Cancer Center, where patients were being treated. Diagnoses of cancers and benign pelvic tumors were based on pathologic review. All blood samples from healthy donors who had no history of cancer were drawn after obtaining informed consent. Blood samples were collected into 8.5-mL vacutainer tubes containing 1.5 mL acid-citrate-dextrose (ACD Solution A Vacutainers; Becton, Dickinson and Company, Franklin Lakes, NJ). Within 60 minutes of blood collection, the addition of 250  $\mu$ L of anti-clumping reagent (CEE-Sure<sup>TM</sup>; Biocept, San Diego, CA) was injected into each tube before being shipped to Biocept and processed within 24 hours of collection. Samples were stored at room temperature (RT) before processing in Biocept's CAP accredited CLIA laboratory.

In the comparison to CellSearch®, three tubes (one CellSave tube and two ACD tubes containing CEE-Sure<sup>TM</sup>) of blood were collected from each of the 93 patients. Given that the CellSearch® assay is FDA-approved for CTC enumeration using only 7.5 mL of blood, only one tube was obtained and delivered to an independent medical laboratory (Genoptix Medical Laboratory, Carlsbad, CA). For our microchannel platform, the overall assay recovery was interpolated between two tubes of blood. Each tube of blood was used to generate a cell pellet for capture within one microchannel. Each microchannel was scored for presence of CTCs based on the standard stain criteria (CK<sup>+</sup>/CD45<sup>-</sup>/DAPI<sup>+</sup>). For the comparison between CellSearch®, the higher total number of CTCs detected in one of two tubes of blood was selected.

A detailed description of CTC capture and detection, FISH, immunofluorescence imaging, statistical analysis and *in vitro*, *ex vivo* and *in vivo* experiments is provided in the Supplementary Methods.

## Supplementary Material

Refer to Web version on PubMed Central for supplementary material.

## Acknowledgments

Portions of this work were supported by the NIH (CA016672, CA 110793, 109298, P50 CA083639, P50 CA098258, CA128797, RC2GM092599, U54 CA151668), the Ovarian Cancer Research Fund, Inc. (Program Project Development Grant), the DOD (OC073399, W81XWH-10-1-0158, BC085265), the Marcus Foundation, the Blanton-Davis Ovarian Cancer Research Program, and the Betty Anne Asche Murray Distinguished Professorship. C.V.P. is supported by a grant from the NCI (T32 training grant CA009666). JBM, RLS, and AMN were supported by the NCI-DHHS-NIH T32 Training grant (T32 CA101642).

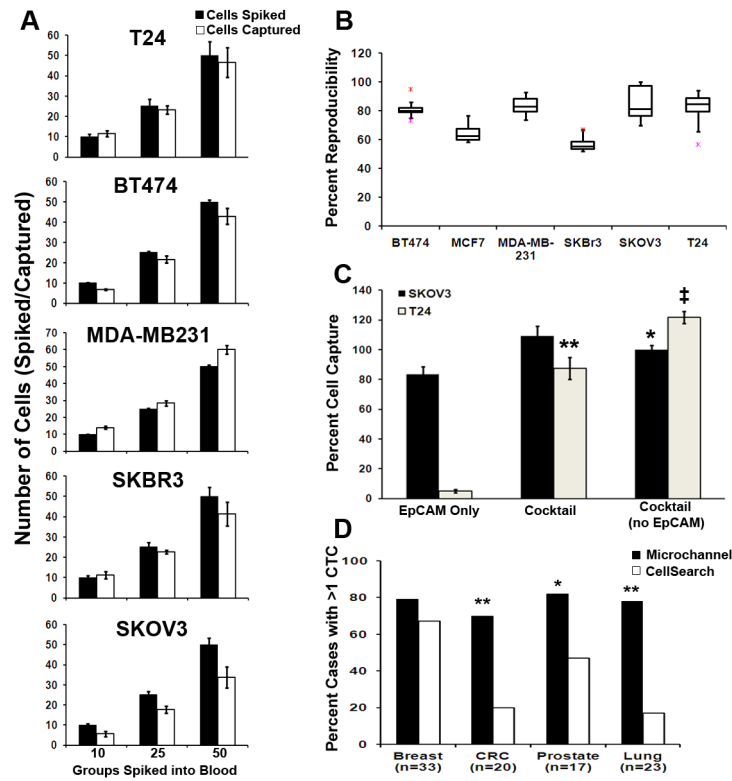
## References

1. Thiery JP. Epithelial-Mesenchymal Transitions in Tumour Progression. *Nature Reviews Cancer*. 2002; 2:442–54.
2. Nagrath S, Sequist LV, Maheswaran S, Bell DW, Irimia D, Ulkus L, et al. Isolation of rare circulating tumour cells in cancer patients by microchip technology. *Nature*. 2007; 450:1235–9. [PubMed: 18097410]
3. Allard WJ, Matera J, Miller MC, Repollet M, Connelly MC, Rao C, et al. Tumor cells circulate in the peripheral blood of all major carcinomas but not in healthy subjects or patients with nonmalignant diseases. *Clinical Cancer Research*. 2004; 10:6897–904. [PubMed: 15501967]
4. Coumans FAW, Doggen CJM, Attard G, de Bono JS, Terstappen LWWM. All circulating EpCAM +CK+CD45– objects predict overall survival in castration-resistant prostate cancer. *Annals of Oncology*. 2010:1–7.
5. Goodman OB Jr, Fink LM, Symanowski JT, Wong B, Grobaski B, Pomerantz D, et al. Circulating Tumor Cells in Patients with Castration-Resistant Prostate Cancer Baseline Values and Correlation with Prognostic Factors. *Cancer Epidemiology Biomarker Prevention*. 2009; 18:1904–13.
6. Cristofanilli M, Budd GT, Ellis MJ, Stopeck A, Matera J, Miller MC, et al. Circulating Tumor Cells, Disease Progression, and Survival in Metastatic Breast Cancer. *New England Journal of Medicine*. 2004; 351:781–91. [PubMed: 15317891]
7. Hayes DF, Cristofanilli M, Budd GT, Ellis MJ, Stopeck A, Miller MC, et al. Circulating Tumor Cells at Each Follow-up Time Point during Therapy of Metastatic Breast Cancer Patients Predict Progression-Free and Overall Survival. *Clinical Cancer Research*. 2006; 12:4218–24. [PubMed: 16857794]
8. Attard G, Swennenhuis JF, Olmos D, Reid AH, Vickers E, A'Hern R, et al. Characterization of ERG, AR and PTEN gene status in circulating tumor cells from patients with castration-resistant prostate cancer. *Cancer Res*. 2009; 69:2912–8. [PubMed: 19339269]
9. Maheswaran S, Sequist LV, Nagrath S, Ulkus L, Brannigan B, Collura CV, et al. Detection of Mutations in EGFR in Circulating Lung-Cancer Cells. *New England Journal of Medicine*. 2008; 359:366–77. [PubMed: 18596266]
10. Fidler IJ, Kim SJ, Langley RR. The Role of the Organ Microenvironment in the Biology and Therapy of Cancer Metastasis. *Journal of Cellular Biochemistry*. 2007; 101:927–36. [PubMed: 17177290]
11. Tarin D, Price JE, Kettlewell MGW, Souter RG, Vass ACR, Crossley B. Mechanisms of Human Tumor Metastasis Studied in Patients with Peritoneovenous Shunts. *Cancer Research*. 1984; 44:3584–92. [PubMed: 6744281]
12. Mego M, Mani SA, Cristofanilli M. Molecular mechanisms of metastasis in breast cancer--clinical applications. *Nat Rev Clin Oncol*. 7:693–701. [PubMed: 20956980]
13. Momburg F, Moldenhauer G, Hämmerling GJ, Möller P. Immunohistochemical study of the expression of a Mr 34,000 human epithelium-specific surface glycoprotein in normal and malignant tissues. *Cancer Research*. 1987; 47:2883–91. [PubMed: 3552208]
14. Ledford H. Cancer theory faces doubts. *Nature*. 2011; 472:273. [PubMed: 21512545]
15. Dickson MN, Tsinberg P, Tang Z, Bischoff FZ, Wilson T, Leonard EF. Efficient Capture of Circulating Tumor Cells with a Novel Immunocytochemical Microfluidic Device. *Biomicrofluidics*. 2011 In Press.

16. Rao CG, Chianese D, Doyle GV, Miller MC, Russell T, Sanders RA Jr, et al. Expression of epithelial cell adhesion molecule in carcinoma cells present in blood and primary and metastatic tumors. *Int J Oncol*. 2005; 27:49–57. [PubMed: 15942643]
17. Fehm T, Muller V, Aktas B, Janni W, Schneeweiss A, Stickeler E, et al. HER2 status of circulating tumor cells in patients with metastatic breast cancer: a prospective, multicenter trial. *Breast Cancer Res Treat*. 2010; 124:403–12. [PubMed: 20859679]
18. Mayr D, Kanitz V, Anderegg B, Luthardt B, Engel J, Löhns U, et al. Analysis of gene amplification and prognostic markers in ovarian cancer using comparative genomic hybridization for microarrays and immunohistochemical analysis for tissue microarrays. *American Journal of Clinical Pathology*. 2006; 126:101–9. [PubMed: 16753589]
19. Camps J, Nguyen QT, Padilla-Nash HM, Knutsen T, McNeil NE, Wangsa D, et al. Integrative genomics reveals mechanisms of copy number alterations responsible for transcriptional deregulation in colorectal cancer. *Genes, Chromosomes & Cancer*. 2009; 48:1002–17. [PubMed: 19691111]
20. Fehm T, Sagalowsky A, Clifford E, Beitsch P, Saboorian H, Euhus D, et al. Cytogenetic Evidence That Circulating Epithelial Cells in Patients with Carcinoma Are Malignant. *Clinical Cancer Research*. 2002;8.
21. Cristofanilli M, Braun S. Circulating tumor cells revisited. *JAMA*. 303:1092–3. [PubMed: 20233831]
22. Aktas B, Tewes M, Fehm T, Hauch S, Kimmig R, Kasimir-Bauer S. Stem cell and epithelial-mesenchymal transition markers are frequently overexpressed in circulating tumor cells of metastatic breast cancer patients. *Breast Cancer Res*. 2009; 11:R46. [PubMed: 19589136]
23. Armstrong AJ, Marengo MS, Oltean S, Kemeny G, Bitting RL, Turnbull JD, et al. Circulating Tumor Cells from Patients with Advanced Prostate and Breast Cancer Display Both Epithelial and Mesenchymal Markers. *Mol Cancer Res*. 2011
24. Hou JM, Greystoke A, Lancashire L, Cummings J, Ward T, Board R, et al. Evaluation of circulating tumor cells and serological cell death biomarkers in small cell lung cancer patients undergoing chemotherapy. *Am J Pathol*. 2009; 175:808–16. [PubMed: 19628770]
25. Kallergi G, Papadaki MA, Politaki E, Mavroudis D, Georgoulas V, Agelaki S. Epithelial to mesenchymal transition markers expressed in circulating tumour cells of early and metastatic breast cancer patients. *Breast Cancer Res*. 2011; 13:R59. [PubMed: 21663619]
26. Moll R, Divo M, Langbein L. The human keratins: biology and pathology. *Histochem Cell Biol*. 2008; 129:705–33. [PubMed: 18461349]
27. Deng G, Herrler M, Burgess D, Manna E, Krag D, Burke JF. Enrichment with anti-cytokeratin alone or combined with anti-EpCAM antibodies significantly increases the sensitivity for circulating tumor cell detection in metastatic breast cancer patients. *Breast Cancer Res*. 2008; 10:R69. [PubMed: 18687126]
28. de Bono JS, Scher HI, Montgomery RB, Parker C, Miller MC, Tissing H, et al. Circulating tumor cells predict survival benefit from treatment in metastatic castration-resistant prostate cancer. *Clin Cancer Res*. 2008; 14:6302–9. [PubMed: 18829513]
29. Stott SL, Hsu CH, Tsukrov DI, Yu M, Miyamoto DT, Waltman BA, et al. Isolation of circulating tumor cells using a microvortex-generating herringbone-chip. *Proc Natl Acad Sci U S A*. 2010; 107:18392–7. [PubMed: 20930119]
30. Woelfle U, Sauter G, Santjer S, Brakenhoff R, Pantel K. Down-regulated expression of cytokeratin 18 promotes progression of human breast cancer. *Clin Cancer Res*. 2004; 10:2670–4. [PubMed: 15102669]
31. Heatley M, Maxwell P, Whiteside C, Toner P. Cytokeratin intermediate filament expression in benign and malignant breast disease. *J Clin Pathol*. 1995; 48:26–32. [PubMed: 7535804]
32. Marrinucci D, Bethel K, Lazar D, Fisher J, Huynh E, Clark P, et al. Cytomorphology of circulating colorectal tumor cells: a small case series. *J Oncol*. 2010; 2010:861341. [PubMed: 20111743]
33. Hayashi N, Nakamura S, Tokuda Y, Shimoda Y, Yagata H, Yoshida A, et al. Prognostic value of HER2-positive circulating tumor cells in patients with metastatic breast cancer. *Int J Clin Oncol*. 2011



34. van de Stolpe A, Pantel K, Sleijfer S, Terstappen LW, den Toonder JM. Circulating tumor cell isolation and diagnostics: toward routine clinical use. *Cancer Res.* 2011; 71:5955–60. [PubMed: 21896640]

**Figure 1.**

Efficiency and reproducibility of cell capture and comparison to CellSearch® technology. (a) Median number of captured carcinoma cells after *ex vivo* spiking of approximately 10, 25, or 50 cells into 10 mL human blood when using the antibody cocktail against cells of varying EpCAM expression. Each spike was performed in triplicate. (b) Percent reproducibility of cell capture after 10 separate *ex vivo* spikes into blood (pink-minimum outlier, red-maximum outlier). (c) Percentages of captured SKOV3 and T24 carcinoma cells after *ex vivo* spiking of approximately 150 cells into 10 mL human blood when using EpCAM antibody only, the antibody cocktail, or the antibody cocktail without the EpCAM antibody. (d) Comparison with the CellSearch® platform for CK+ CTCs captured from patients with breast, colorectal, lung, or prostate carcinomas. *a*: Tumor types approved for CTC enumeration using CellSearch®, *b*: For samples from breast, colorectal and lung cancer patients, the antibody cocktail (AC15) composed of 10 monoclonal antibodies was used, *c*: For samples from prostate cancer patients, the antibody cocktail (AC16) composed of 11 monoclonal antibodies was used. \* $P < 0.05$ , \*\*  $P = 0.001$ , ‡  $P = 0.0001$ .

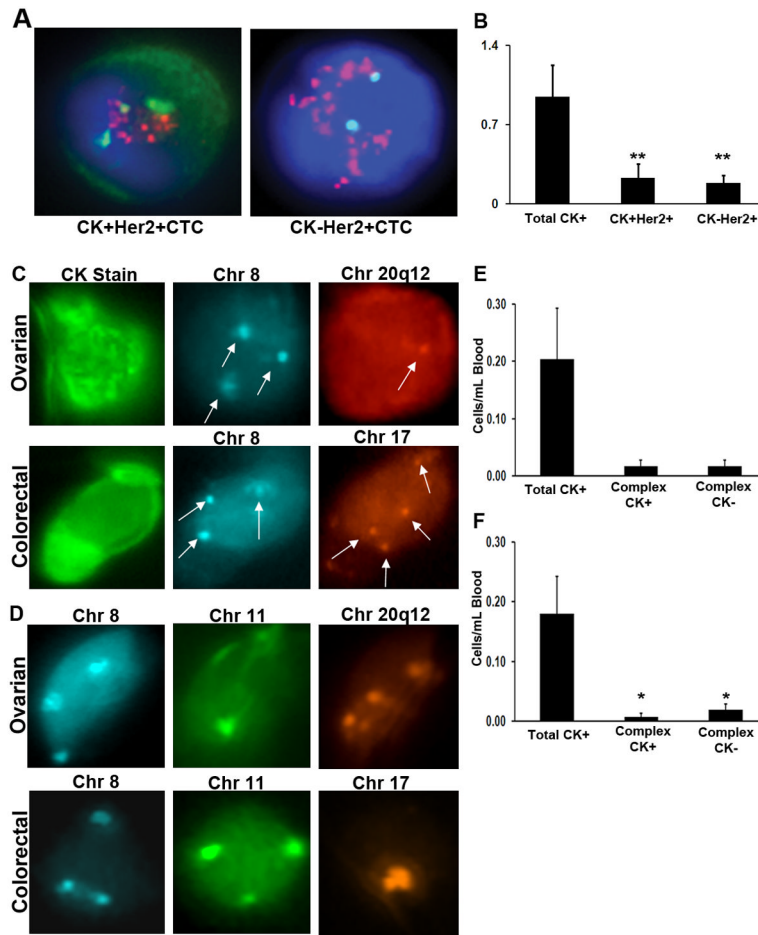


**Figure 2.**

Capture of CK+ and CK- complex aneuploid CTCs in breast, ovarian or colorectal cancers. (a) Representative images illustrating detection of HER2+/CK+ and HER2+/CK- CTCs. Both cells display a  $>2.2$  *HER2*/Centromere 17 ratio, confirming positive *HER2* amplification. (b) Comparison of total CK+/CD45-, CK+/CD45-/HER2+ and CK-/CD45-/HER2+ cells from advanced-stage breast cancer patients. (c) Capture of circulating ovarian (top) and colorectal (bottom) carcinoma cells that stain for cytokeratin. Subsequent FISH shows an ovarian cancer cell with trisomy in chromosome 8 (blue) and monosomy in region 20q12 (red), whereas the colorectal cancer cell has trisomy in chromosome 8 and tetrasomy in chromosome 17 (orange, arrows). (d) Capture of CK-negative circulating ovarian (top) and colorectal (bottom) carcinoma cells. FISH of an ovarian cancer cell with trisomy in chromosome 8 (blue), monosomy in chromosome 11 (green), and tetrasomy in region 20q12 (orange), whereas the colorectal cancer cell has trisomy in chromosomes 8 (blue) and 11 (green) and monosomy in region 20q12. The average number of total cytokeratin, complex aneuploid cytokeratin-positive, and cytokeratin-negative circulating tumor cells per milliliter of blood is shown for (e) ovarian and (f) colorectal cancer patients. \* $P < 0.05$ , \*\* $P = 0.007$ .

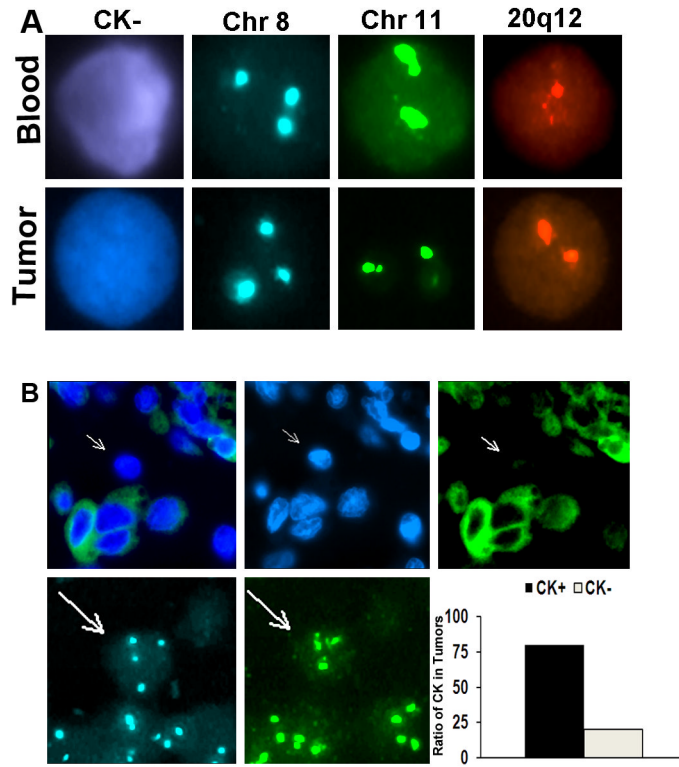


**Figure 3.** Matched CK-positive and negative cells in circulation and primary tumor. (a) CK-negative ovarian cancer cells identified in circulation (top) at the time of surgical resection have similar aneuploidy as regions in the tumor (bottom). Represented are cells with trisomy of chromosome 8. (b) CK staining of ovarian carcinoma samples reveals CK-negative cells with aneuploidy (arrows) similar to those detected in circulation. Approximately 20% of the tumor had such CK-negative cells.

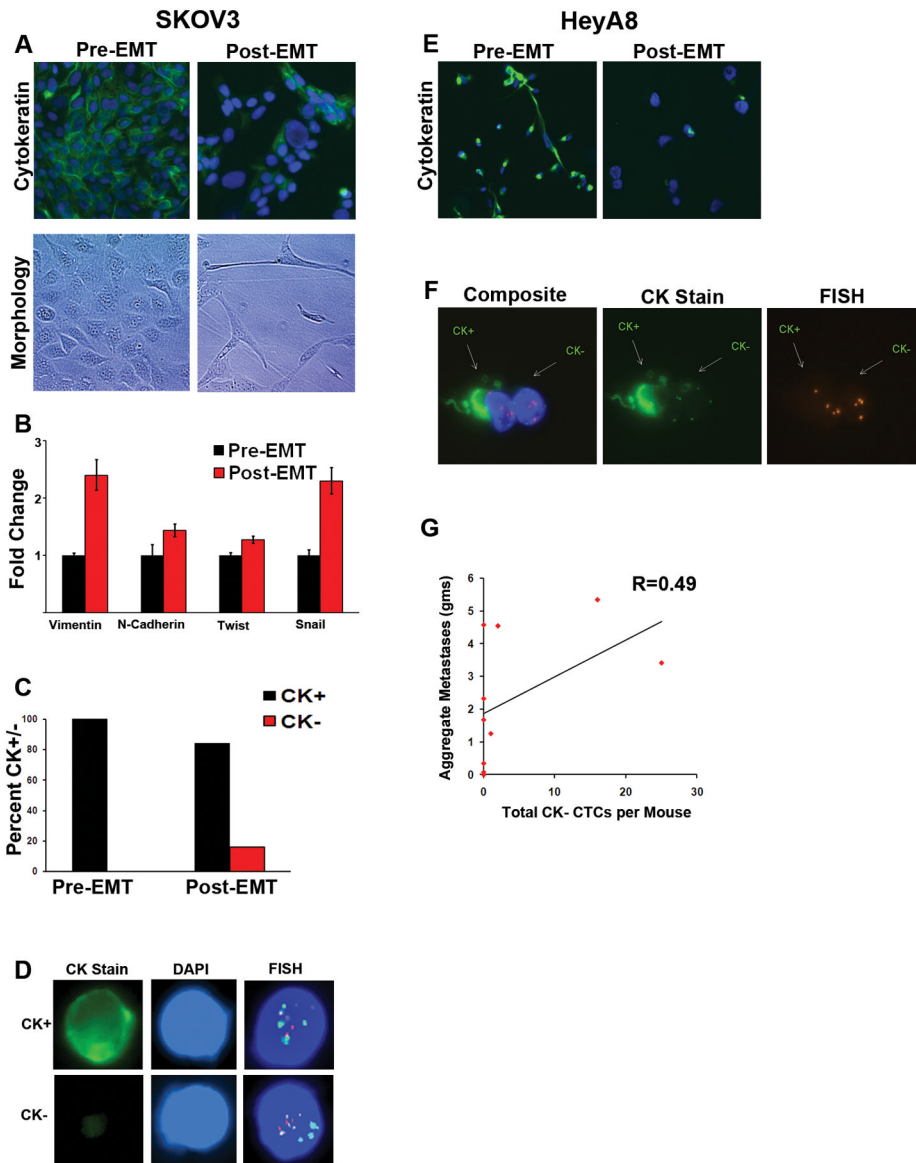


**Figure 4.** Characterization and capture of cytochrome-negative cells after induction of EMT. **(a)** SKOV3 cells were either grown in regular culture media (Pre-EMT) or in serum-free media with 10 ng/mL TGF- $\beta$  (Post-EMT) for 72 hours. Pictured are representative immunofluorescent images (top) of Pre-EMT cells demonstrating 100% CK expression and areas of Post-EMT cells with absent CK expression. Approximately 20% of post-EMT cells were found to have complete loss of cytochrome expression. Phase contrast images of the same cells (bottom) demonstrate a morphologic change characteristic of EMT. **(b)** Quantitative real-time PCR for markers of EMT of SKOV3 cells with and without TGF- $\beta$  treatment for 72 hours. **(c)** Following 72 hours, pre- and post-EMT cells were spiked *ex vivo* into mouse blood and run through the CEE<sup>TM</sup> microchannel. All pre-EMT cells that were captured were CK+ and had complex aneuploidy, while 16% of post-EMT cells were CK- and had similar complex aneuploidy. The bar graph represents ratios of CK+ and CK- complex aneuploid captured cells in each group. **(d)** Representative images of CK+ and CK- complex aneuploid SKOV3 cells are shown from within the microchannel. **(e)** HeyA8



cells were cultured in regular media (Pre-EMT) or serum-free media with 10 ng/mL TGF- $\beta$ (Post-EMT) for 72 hours. Representative immunofluorescent images of Pre-EMT cells demonstrating nearly 100% CK expression and TGF- $\beta$  treated cells with absent CK expression are shown. Approximately 60% of TGF- $\beta$  treated cells were found to have complete loss of cytokeratin expression. **(f)** HeyA8 cells were injected into 10 mice to establish a metastatic ovarian model. Once moribund, blood was collected from each mouse by cardiac puncture. Pictured are a CK+ and CK- CTC within the microchannel demonstrating hyperploidy of chromosomes 11 and 17. **(g)** Correlation of total aggregate tumor burden with enumeration of complex aneuploid CK- CTCs by mouse.